Available online at www.sciencedirect.com
SCIENCE DIRECT®
Polymer 44 (2003) 4389–4403
polymer
www.elsevier.com/locate/polymer

Feature Article

Recent developments in the formation, characterization, and simulation of micron and nano-scale droplets of amorphous polymer blends and semi-crystalline polymers

Bobby G. Sumpter[a,*], Donald W. Noid[a], Michael D. Barnes[b]

[a]*Computer Science and Mathematics Division, Oak Ridge National Laboratory, P.O. Box 2008, One Bethel Valley Road, Oak Ridge, TN 37831, USA*
[b]*Chemical Science Division, Oak Ridge National Laboratory, Oak Ridge, TN 37831, USA*

Received 25 April 2003; received in revised form 13 May 2003; accepted 13 May 2003

Abstract

Polymer micro- and nano-particles are fundamental to a number of modern technological applications, including polymer blends or alloys, biomaterials for drug delivery systems, electro-optic and luminescent devices, coatings, polymer powder impregnation of inorganic fibers in composites, and are also critical in polymer-supported heterogeneous catalysis. In this article, we review some of our recent progress in experimental and simulation methods for generating, characterizing, and modeling polymer micro- and nano-particles in a number of polymer and polymer blend systems. By using instrumentation developed for probing single fluorescent molecules in micron-sized liquid droplets, we have shown that polymer particles of nearly arbitrary size and composition can be made with a size dispersion that is ultimately limited by the chain length and number distribution within the droplets. Depending on the time scale for solvent evaporation—a tunable parameter in our experiments—phase separation of otherwise immiscible polymers can be avoided by confinement effects, producing homogeneous polymer blend micro- or nano-particles. These particles have tunable properties that can be controlled simply by adjusting the size of the particle, or the relative mass fractions of the polymer components in solution. Physical, optical, and mechanical properties of a variety of micro and nano-particles, differing in size and composition, have been examined using extensive classical molecular dynamics calculations in conjunction with experiments to gain deeper insights into fundamental nature of their structure, dynamics, and properties.

Keywords: Polymer blends; Micro- and nano-particles; Micro droplets

1. Introduction

Enormous commercial and scientific attention has been and continues to be focused on multi-component polymer systems as a means for producing new materials on the micron and nanometer scale with tailored material, electrical and optical properties. Composite polymer particles or polymer alloys with specially tailored properties could have many novel uses in electro-optic and luminescent devices [1–3], thermoplastics [4] and conducting materials [5,6], hybrid inorganic–organic polymer alloys [7], and polymer-supported heterogeneous catalysis [8]. However, the vast majority of this large body of work is based on thin-film processing (1-D confinement), or self-assembly processes—for example in co-polymer systems [9]. In the latter approach, spontaneous self-assembly of co-polymeric systems to form micellar, cylindrical, or lamellar morphologies depends on the solvent, and nature of the co-polymer system [10–13]. This is a rich area of study that has attracted the attention of many groups. However, self-assembly of copolymer systems, for example, in nano-spherical micellar structures typically favors length scales on the order of a few nanometers. For many optical applications, one is interested in periodicity on the order of hundreds of nanometers (i.e. photonic bandgap structures), as well as active control over individual particle size and position.

Recently, we have explored ink-jet printing methods for producing polymer particles with arbitrary size and composition. This method is based on using droplet-on-demand generation to create a small drop consisting of a polymer mixture in some solvent [14,15]. As the solvent evaporates, a polymer particle is produced whose size is defined by the initial size of the droplet (typically between 5 and 30 μm),

* Corresponding author.

0032-3861/03/$ - see front matter © 2003 Published by Elsevier Science Ltd.
doi:10.1016/S0032-3861(03)00428-2

and the weight fraction of polymer (or other non-volatile species) in solution. Because the droplets are produced with small excess charge during ejection from the nozzle, this approach lends itself naturally to spatial manipulation of micro- and nano-particles using electrodynamic focusing techniques [16]. These particles in the micro- and nanometer size range provide many unique properties due to size reduction to the point where critical length scales of physical phenomena become comparable to or larger than the size of the structure. Applications of such particles take advantage of high surface area and confinement effects, leading to interesting nano-structures with different properties that cannot be produced using conventional methods. Clearly, such changes offer an extraordinary potential for developing new materials in the form of bulk, composites, and blends that can be used for coatings, opto-electronic components, magnetic media, ceramics and special metals, micro- or nano-manufacturing, and bioengineering. The key to beneficially exploiting these interesting materials and technology is a detailed understanding of the connection of nano-particle technology to atomic and molecular origins of the process. The present article is a review of our work over the past several years on both experimental and computational approaches for generation, characterization, and analysis of polymer micro and nano-particles.

2. A new approach to generation and analysis of monodisperse polymer particles

Over the last several years, advances in microdroplet production technology for work in single-molecule detection and spectroscopy in droplet streams has resulted in generation of droplets as small as 2–3 μm with a size dispersity of better than 1% [14]. In the context of polymer particle generation, droplet techniques are attractive since particles with a high degree of size and material homogeneity control can be starightforwardly produced in this way [17,18]. In a similar spirit, work by Davis and co-workers, Ray and others have pursued in situ polymerization techniques by irradiating micron-droplets of monomer solution. While droplet production in the size range of 20–30 μm (diameter) is more or less routine (several different on-demand droplet generators are now available commercially), generation of droplets smaller than 10 μm remains non-trivial especially under the added constraint of high monodispersity. Small droplets (<10 μm) are especially attractive as a means for producing multi-component polymer blend and polymer-composite particles from solution since solvent evaporation can be made to occur on a time scale that is much shorter than the characteristic polymer-self-organization or diffusion time-scales, thus inhibiting phase-separation in these systems. This implies time scales for particle drying on the order of a few milliseconds and droplet sizes <10 μm (depending on solvent, droplet environment, etc.). We have shown recently that a microdroplet approach can be used to form homogeneous composites of co-dissolved bulk immiscible polymers using instrumentation developed in our laboratory for probing single fluorescent molecules in droplet streams [19]. In addition to a new route to forming nano-scale polymer composites, a microparticle format offers a new tool for studying multi-component polymer blend systems under three-dimensional confinement in the absence of substrate interactions.

Several different choices exist for producing micron and sub-micron-droplets of solution—each with certain trade-offs in terms of volume throughput, nominal size, and size dispersity. There are additional trade-offs associated with sampling and interrogation facility that should be considered as well. Two familiar methods of droplet production include electrospray generation and aerosol generation using a vibrating orifice coupled to a high-pressure liquid stream. In electrospray generation, a liquid stream is forced through a needle biased at approximately 1 kV (nom.). Charge-carriers induced on the surface of the liquid stream eventually come close enough during solvent evaporation for Coulomb repulsion to occur (the Taylor cone), resulting in fragmentation, or explosion, of the liquid stream. This results in a cloud of charged liquid droplets whose size can be made quite small (<1 μm). The obvious drawback is that it is difficult to isolate individual particles for study, and size dispersity tends to be highly sensitive to experimental parameters.

Another common method of producing liquid droplets is the technique of vibrating orifice aerosol generation (VOAG). Invented by Berglund and Liu back in the 1970s, the VOAG is unmatched in terms of volume throughput (>100 nanoliters per second) and size dispersity (<0.1% depending on experimental conditions). This technique works by introducing a high-frequency (10–100 kHz) instability in a high-pressure liquid stream applied by a piezoelectric transducer (PZT). The resulting fragmentation of the stream produces highly monodisperse droplets that are ultimately limited by the purity of the RF signal applied to the PZT. Some disadvantages of this mode of production are that the droplets travel at high speeds (several meters/second), and are quite close together (typically not more than 3 droplet diameters apart). This makes isolation and spectroscopic interrogation of individual droplets difficult. A more serious problem is in the significant particle size limitations associated with this technique. A VOAG works best at a size range of 30–50 μm, but can function down to about 12–15 μm. Because of the way droplets are produced, however, there is a concomitant increase in the RF frequency that can be problematic.

The method we have chosen in our experiments is an 'on-demand' or droplet ejection device [19]. Like a VOAG, it also uses piezoelectric transduction but at much lower frequencies. The physics of droplet production is completely different for

the two methods: The VOAG operates by generating a high (and fixed) frequency instability in a liquid stream; the on-demand droplet generator functions by the application of a acoustic wave to a static solution, which forces (ejects) a droplet out of a micron-sized orifice. We use Pyrex or quartz tubing that is heated, drawn, cut and polished to produce a tapered orifice that can range in size from 1 to 50 μm. The droplet sizes are comparable (usually slightly larger) to the orifice diameter and, depending on the quality of the orifice, size dispersity less than 1% can be achieved. Droplet production rates tend to be significantly lower than the forementioned techniques. Ultimately, droplet rates are limited by piezoelectric relaxation times (10 kHz); practically, however, under conditions of high monodispersity, droplet rates are typically much lower (20–100 Hz). The advantages of this technique are small size and on-demand production that makes single droplet/particle manipulation and interrogation straightforward.

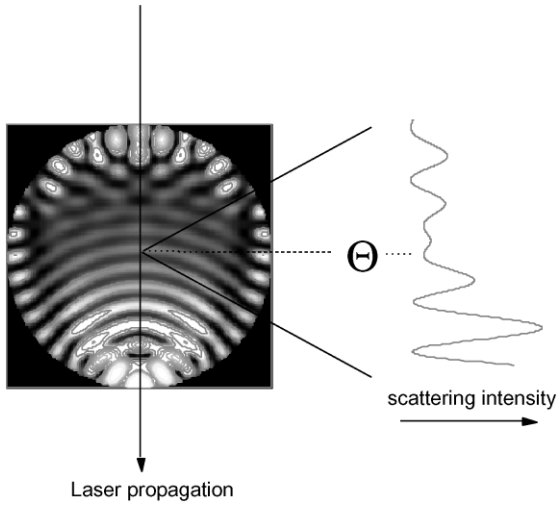

Fig. 1. Schematic of electric field intensity distribution in the equatorial plane for a vertically polarized input plane wave on a dielectric sphere with size parameter (diameter/wavelength) of 20. The light collimation optics subtend a plane angle, Θ, and the scattered intensity as a function of Θ (for given ϕ) is represented on the right.

3. 2-D Light scattering

Several groups have explored optical probes of polymer phase separation and domain ordering in thin films. For micro-phase separation (with domain sizes in the order of 1–10 μm) conventional phase-contrast, differential interference contrast, or scanning confocal microscopy techniques are sufficient to image the sample with (diffraction-limited) spatial resolution that is small compared to the domain size. For higher resolution imaging, novel non-linear and scanning near-field optical probes have been used as well. These techniques are well suited for thin-film formats but are less useful for probing phase structure within a three-dimensional system larger than a few optical wavelengths. Our approach for probing phase-separation and material homogeneity in polymer composites is essentially an interferometric technique that has been used for a number of years as a method for sizing liquid microdroplets (size range 2–20 μm. Recently, this measurement technique has been used to recover information on drying kinetics, inter-polymer dynamics, and material properties such as dielectric constant. The basis of the technique involves first production and electrodynamic levitation of a single polymer, or polymer blend microparticle, then illuminating the microsphere with a plane-polarized laser to produce an inhomogeneous electric field intensity distribution, or grating, within the particle shown in Fig. 1. This nodal pattern, well known in the aerosol physics community, results from interference between refracted and totally-internally-reflected waves within the particle. The angular spacing between intensity maxima, as well as the intensity envelope is a highly sensitive function of particle size and refractive index (both real and imaginary parts).

Two-dimensional diffraction (or, angle-resolved scattering) is sensitive to material homogeneity on a length scale of $\lambda/20$ or about 20–30 nm for optical wavelengths [20], and has also been used to probe dynamics of cluster formation [21], and structural anisotropy in polymer-inorganic nanoparticle aggregates. This dimension is comparable to single-molecule radii of gyration for relative large molecular weight (>100 k) polymers, and thus provides molecular scale 'resolution' of material homogeneity in ultra-small volumes (1–100 femtoliters), although not in a real-space sense. Inversion of the Fourier-plane intensity pattern to obtain a real-space map of refractive index fluctuations is non-trivial and has been explored theoretically by a number of groups. In many cases, however, the qualitative information provided by contrast in intensity fringes and agreement with Mie calculations is useful to distinguish between 'homogeneous' and 'inhomogeneous' without specific reference to actual internal phase structure.

Fig. 2 shows an example of typical 2-D angular scattering (or diffraction) from a single levitated polyethylene glycol microparticle (≈6 μm diameter). One-dimensional fringe patterns (intensity vs. azimuthal angle ϕ) are obtained simply by extracting a specific row from the 2-D matrix of intensity points accumulated with a CCD camera. In our experimental configuration, this intensity grating is projected in the far-field using (f/1.5) collimating optics and detected with a cooled 16-bit CCD camera. The scattering angle (center angle and width) is established by means of an external calibration, and is used for high-precision Mie analysis of one-dimensional diffraction data [22]. For optical diffraction studies, individual particles were studied using droplet levitation techniques. Details of the apparatus and CCD calibration procedure are described in Ref. [22]. The nominal scattering angle was 90 degrees with respect to the direction of propagation of the vertically polarized

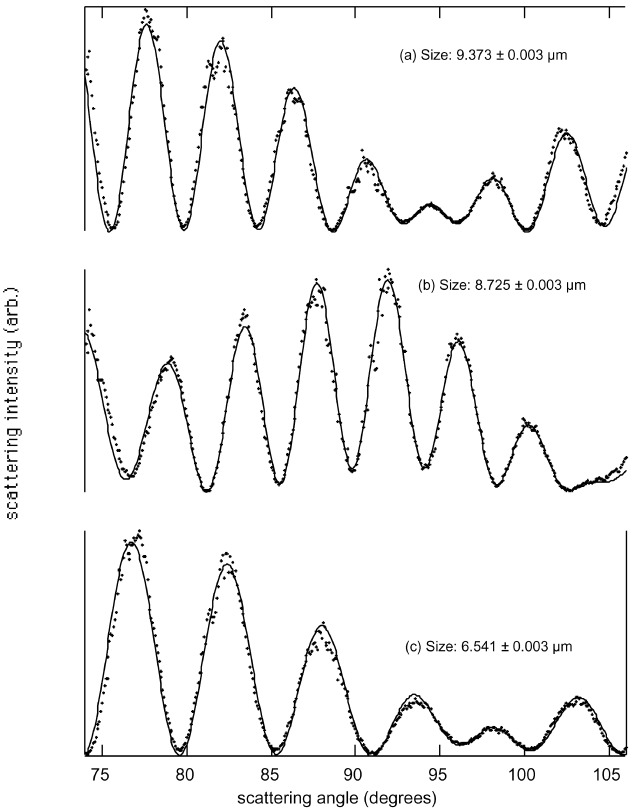

Fig. 2. Representative 1-D fringe patterns (scattered intensity as a function of angle in the equatorial plane) for three different levitated polyetheylene glycol microspheres. The 2-σ uncertainly in size determination is dependent on size but is typically about 5 nm.

HeNe laser, and the useable full plane angle (defined by the $f/1.5$ achromatic objective) was 35 degrees.

An important application of this technique is the study of phase-separation behavior in mixed-polymer systems under three-dimensional confinement. The use of optical diffraction in spherical dielectric particles as a probe of material homogeneity in polymer composites, and its limitations of domain size (in multi-phase composites) and dielectric constant are relatively new in polymer science. We have successfully used this measurement technique to recover information on drying kinetics, inter-polymer dynamics, and material properties. Latter we describe results of detailed molecular dynamics (MD) modeling that can be used to connect experimental observations with microscopic dynamics within a polymeric particle.

Composite polymer particles, or polymer alloys, with specifically tailored properties could find many novel uses in a number of fields. However, the problem of phase separation from bulk-immiscible components in solution often poses a significant barrier to producing many commercially and scientifically relevant homogeneous polymer blends [23–25]. The typical route taken in trying to form homogeneous blends of immiscible polymers is to use compatibilizers to reduce interfacial tension. Recently, a number of different groups have examined phase-separation in copolymer systems to fabricate fascinating and intricate meso- and micro-phase separated structures with a rich variety of morphologies.

Our interest focuses on trying to suppress phase-separation in mixed polymer systems by very rapid solvent evaporation from small (≤ 10 μm diameter) droplets of dilute polymer solution. Using instrumentation developed in our laboratory for probing single fluorescent molecules in 1–10 μm diam. droplet streams [26], we have been exploring use of microdroplets to form homogeneous polymer composites without compatibilizers as a possible route to new materials with tunable properties [27]. The primary condition for suppression of phase separation in these systems is that solvent evaporation must occur on a time scale that is fast compared to self-organization times of the polymers. This implies time scales for particle drying on the order of a few milliseconds implying droplet sizes ≤ 10 μm (depending on solvent, droplet environment, etc.). In addition to a new route to forming nano-scale polymer composites, a microparticle format offers a new tool for studying multi-component polymer blend systems in confined to femtoliter and attoliter volumes where high surface area-to-volume ratios play a significant role in phase separation dynamics.

Fig. 3 shows qualitatively the effect of phase-separation on fringe contrast and definition for two polymer blend particles prepared from different sized droplets of co-dissolved polymers (polyvinyl chloride and polystyrene) in tetrahydrofuran (THF). The particle on the left is homogeneous as evidenced by uniform fringe intensity, and high-fringe contrast and definition. Moreover, the scattering data can be matched quantitatively to Mie theory calculations that assume a homogeneous particle. The particle on the left has no discernible fringe structure, but does display interesting periodic ‘island’ structure implying some order and uniformity of phase-separated domains.

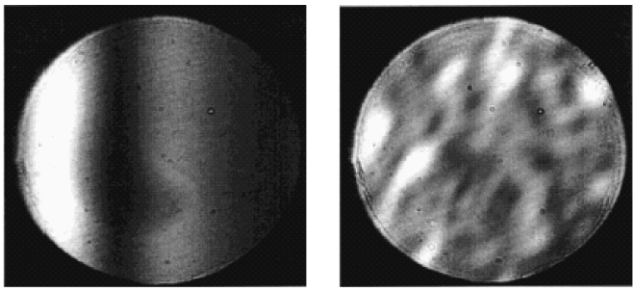

Fig. 3. Two-dimensional angle-resolved diffraction patterns from polystyrene/polyvinyl chloride blend particles (50:50 mass fraction). The pattern on the left is a 2.5 μm diameter particle prepared from a 10 μm droplet of polymer solution in THF, the particle on the right is about 12 μm in diameter formed from a droplet about 35 μm in diameter. The evaporation time scale for the larger droplet is about a factor of 3 longer than that of the smaller one, allowing sufficient time for self-organization within the particle. The phase-separation for the larger particle is manifested in the complete loss of well-defined diffraction fringes as the phase-separated domains act as scattering centers within the particle. From Ref. [15].

Fig. 4 shows MD simulations of a stable polymer blend particle (10 nm diameter) composed of immiscible components. The leftmost particle remains homogeneous throughout a broad temperature range. For phase separation to occur (right), an enormous amount of thermal energy must be supplied in order to overcome the surface energy barrier. This result agrees qualitatively with the observation that homogeneous blends of bulk-immiscible polymers can be formed in spherical microparticles. The composite particle was calculated to have a single melting temperature of 190 K and glass transition temperature of 90 K which is different than either of the polymer components (T_m) 218 K, T_g) 111 K for light and T_m) 162 K, T_g) 81 K for dark). The segregated particle has two melting points and glass transition temperatures that correspond to within 10 K of the individual components.

Formation of homogeneous polymer blend composites from bulk-immiscible co-dissolved components using droplet techniques has two requirements. First, solvent evaporation must occur on a relatively short time scale compared to polymer translational diffusion. Second, the polymer mobility must be low enough so that, once the solvent has evaporated, the polymers cannot overcome the surface energy barrier and phase-separate. We have previously shown definitively the effects of droplet size and solvent evaporation, and the second requirement is almost always satisfied even for modest molecular weight polymers. To explore effects of polymer mobility in detail, we looked at composite particles of PEG oligomers (M_W 200, 400, 1000, and 3400) with medium molecular weight (14 k) atactic poly(vinyl alcohol) (PVA). This system allows us to systematically examine the phase separation behavior where one component (PEG) has substantially different viscosities (specified as 4.3, 7.3, and 90 cSt at room temperature for PEG, PEG, and PEG, respectively).

We observed that the higher molecular weight PEG polymer blend particles are homogeneous as determined from bright-field microscopy, optical diffraction, and fluorescence imaging. Blend particles prepared with the 200 molecular weight PEG were observed to form sphere-within-a-sphere particles with a PVA central core. Fig. 5 shows diffraction data acquired from particles at successive 10 min intervals from a 10 μm diameter PEG[200]/PVA[14 k] (80:20 w/w) particle. As shown in the first frame, the particle is initially homogeneous. The second and third frames indicate that the composite particle undergoes phase separation into an inhomogeneous particle as evidenced by the fringe distortion. Interestingly, the structure in the 2D diffraction data for this system is much different than those observed for large phase-separated PVC/PS particles that presumably coalesce into submicron spheroidal domains. On the basis of fluorescence and phase-contrast imaging data, PEG[200]/PVA[14 k] particles form spherically symmetric (sphere-within-a-sphere) heterogeneous structures, which should also produce well-defined diffraction fringes. Our interpretation of these data is that diffusional motion of the PVA core in the PEG host particle, combined with rotational diffusion of the particle, breaks the spherical symmetry and thereby introduces distortion in the diffraction pattern. This observation is entirely consistent with our model of polymer-composite formation where heterogeneous particles may be formed provided that the mobility of one of the polymers is low enough to overcome the surface energy barrier. From the 20 min time scale for phase separation in the low molecular weight PEG system, we estimate a diffusion coefficient of 10^{-10} cm^2/s, which is consistent with recent molecular modeling results. For a diffusion coefficient, D, of 10^{-10} cm^2/s and 1200 s time scale, the average diffusion distance $r = (6Dt)^{1/2} = 8.5. \times$ μm, which is comparable to the particle diameter. Composite particles formed from the higher molecular weight PEG (>1000) form homogeneous composite particles with PVA.

Another interesting aspect of this work comes from Mie analysis of the scattering data for homogeneous composite particles. Our observation for several different polymer blend systems is that the material dielectric constant (manifested in both the real and imaginary parts of the refractive index) can be tuned by adjusting the relative weight fractions of the polymers in the mixture. Both Re(n) and Im(n) for the polymer blend microparticles are intermediate between the values determined for pure single-component particles and can be controlled by adjusting the weight fractions of polymers. For both

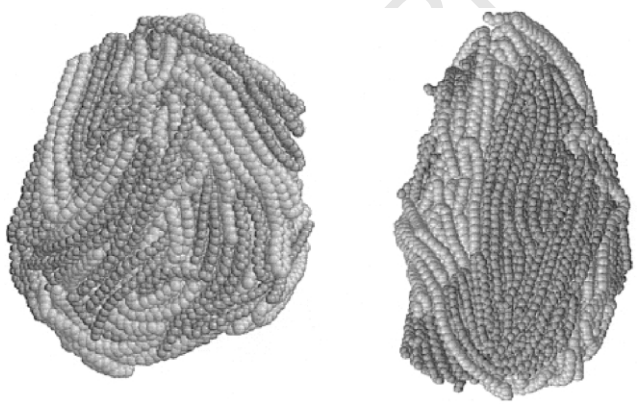

Fig. 4. Calculated structures for homogeneous (left) and phase segregated (right) 10 nm polymer blend particles.

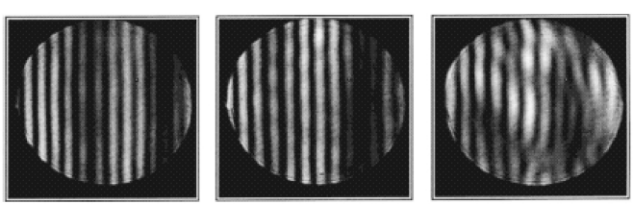

Fig. 5. Two-dimensional diffraction data acquired at successive 10 min intervals from a 10 μ diameter PEG/PVA particle (Ref. [15]).

miscible and (bulk) immiscble polymers that we have combined in homogeneous microparticles, we observe the measured refractive index to be very close to estimates obtained from a simple mass-weighted average of the two species.

Although the microdroplet technique is well suited for producing nearly arbitrarily small particles (down to a single molecule limit), optical diffraction (which requires particle sizes on the order of a few optical wavelengths) is obviously not suitable for probing particles smaller than a few hundred nanometers. To complement our experimental effort on larger sized particles, we have also investigated various dynamical and steady-state properties of much smaller polymer and polymer blend nano-particles (1–10 nm diameter) using MD tools. These simulations allow development of some insight into the structure, and properties of polymer blend particles, as well as aiding in interpretation of experimental results and guiding future experiments. Using classical MD techniques, we have examined polymer nano-particles of varying size (up to 300,000 atoms), chain lengths (between 1 and 200 monomers), and intermolecular interaction energy allowing the systematic study of size-dependent physical properties and time dependence of segregation/equilibration of these particles [28]. These results are discussed in more detail in latter sections of this review.

3.1. Novel polymer particle structures: photonic molecules

For many years, researchers in materials and photonics have been interested in the design and fabrication of structures that confine and manipulate electromagnetic fields on length scales comparable to optical wavelengths. The ultimate goal is an all-optical information processing and computation platform using photons in ways analogous to electrons in silicon devices on similar length scales. Specific focus-areas such as wafer-scale integration, parallel processing and frequency management (e.g. add-drop filters), on micron- or sub-micron length scales are active areas of photonics research. While a great deal of progress has been made in the burgeoning field of *microphotonics*, we are still a long way off from realizing important goals such as the optical transistor, and all-optical integrated circuits [29].

One of the critical issues faced by researchers trying to engineer high-density photonic device and optical computing/information processing structures is the problem of 'turning' the path of the photon. Waveguide structures work well as long as the path is straight, however, including turns with bend radii comparable to propagation wavelength is seriously problematic since the losses tend to be unacceptably high. Typically, minimum bend radii in such structures are on the order of several tens of microns (at least) to avoid scattering and retro-reflection losses at the turn. Recently a new strategy has emerged for confining and manipulating electromagnetic fields with precise frequency and spatial control. Based on coupled optical microcavities, these new photonic structures have been called photonic molecules by virtue of the similarity between the field eigenmodes and electronic structure in real molecules [30]. In contrast with waveguides in PBG crystals (fabricated by introducing line defects) where a broad range of frequencies are allowed to propagate within the bandgap, photonic molecule/polymer structures permit transmission only near cavity resonance frequencies. Furthermore because the resonance Qs (energy storage factors) can be made quite high ($>10^4$), it is conceivable that these kinds of structures can function as amplifiers, switches, and add-drop filters.

Recently, we discovered an interesting material property of a simple water-soluble polymer blend that allowed us to realize a new kind of polymer microsphere-based structure that we called photonic *polymers* [31]. In the course of screening different water-soluble polymer blends for high-density ordered microsphere array applications [32], we found that particles made from polyethylene glycol ($\approx$10 K M_W) and polyvinyl alcohol (14 K M_W) in a 4:1 mass ratio had a tendency to stick together in clumps of twos, threes, or multiple particles. Under higher magnification, we observed that the 'sticking' was in fact a partial merging of the particle surfaces shown in Fig. 6. The particle binding was so robust, that under high-precision particle focusing conditions, we were able to 'stack' particles in nearly perfect columnar structures up to $\approx$20 particles high. Other types of two- and three-dimensional architectures were

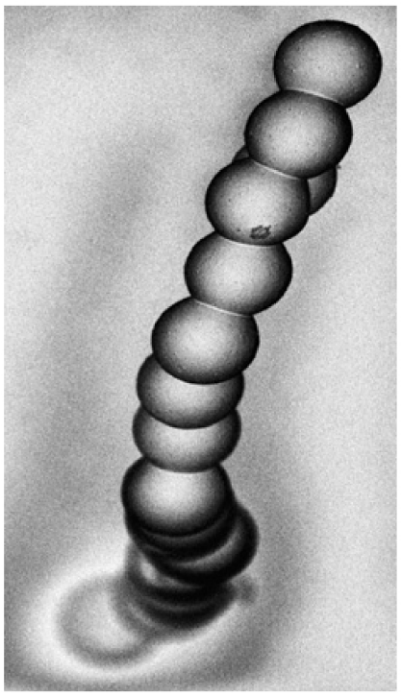

Fig. 6. Electron micrograph of a photonic polymer structure made from merged polymer blend microspheres (Ref. [31]). There are about 30 individual spheres in the vertical chain that has folded near the top.

explored using an electric quadrupole and computer-controlled 2-D translation stage for particle positioning.

One of the most surprising aspects of this work was the observation of sharp resonance features (distinct from 'monomer' resonances) in fluorescence from dye doped into the particles. Interestingly, the optical properties of merged-sphere systems shown in Fig. 6 were considered theoretically several years earlier by Videen and co-workers [33]. Resonance features in emission were also observed in transient merging-droplet experiments by Moon et al. [34]. What is surprising about the observation of shared optical resonances from merged spheres (especially with the large solid angle of intersection) is that a large segment of the dielectric boundary which confines the electromagnetic wave has been removed. Geometric optics calculations of long-lived trajectories in merged spheres show clearly that high-Q resonances are *not* supported for (plane) angles of intersection exceeding more than a few degrees. Calculations on bisphere of differing sizes have shown interesting antinodal structure that includes an interaction between states with significantly different angular momenta, but with very low-Q. Only in the special case where the contact angle is very small-similar to the physisorbed sphere case, are high-Q coupled resonances in the equatorial plane supported.

In our experimental case, typical plane angles of intersection can be more than 50 degrees, yet the structures clearly support high-Q resonances. Using a combination of three-dimensional ray optics and surface-of-section techniques [35], we were able to find robust periodic trajectories that make a quasi-helical path around the particle chain axis. Fig. 6 shows a schematic of a photonic molecule mode for a tri-sphere system with an angle of intersection similar to the experimental case (upper), and an example of a long-lived periodic trajectory that couples three merged spheres with a solid angle of intersection of ≈ 0.3 sr (plane angle of 40°). These coupled resonances appear to be highly robust with respect to overlap angle, deviations from collinearity, and size along the chain axis. The classical path shown in Fig. 7 could be interpreted as connecting azimuthal modes of the same index ($0 \leq m \leq n$, $n \approx X = \pi d/\lambda$) with opposite sign [36].

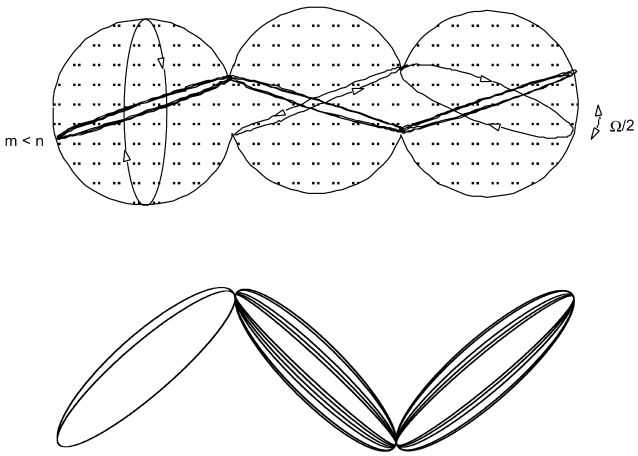

Fig. 7. Ray path schematic (upper) and 3-D periodic trajectory in a linear tri-sphere. The plane angle of intersection was chosen to be 20°, close to the experimental case shown in Fig. 6 (Ref. [35]).

4. Computational modeling and simulation

Molecular modeling provides an efficient method for visualizing processes at a sub-macromolecular level that also can be used to connect theory and experiment. Particularly attractive from a computational point of view, is that polymer particles are very close to the size scale where a complete atomistic model can be studied without using artificial constraints such as periodic boundary conditions, yet these particles are too small for traditional experimental structure/property determination. Polymeric particles in the nano- and micrometer size range show many new and interesting properties due to size reduction to the point where critical length scales of physical phenomena become comparable to or larger than the size of the structure itself. This size-scale mediation of the properties (mechanical, physical, electrical, etc.) opens a facile avenue for the production of materials with pre-designed properties [37,38]. In order to develop a molecular-level understanding of how the various properties are influenced by the size-scale of the material, we developed a number of computational techniques that allowed us to examine the structure and dynamics of these interesting new materials [39–41].

The primary tool used was a MD-based computational algorithm for generating and modeling polymer nanoparticles which leads to particles that are as similar as possible to the experimentally created polymer particles [41]. MD is an invaluable tool to study structural and dynamical details of polymer processes at the atomic or molecular level and to link these observations to experimentally accessible macroscopic properties of materials. Methods of MD are, of course, well known; one needs to solve Hamilton's equations (or any other formulation of the classical equations of motion) starting from some initial positions and momenta of all of the atoms in the system and propagating the solution in a series of time steps. However, the large number of coupled equations of motion necessarily required for treating a nano-scale polymeric system is seriously problematic in most conventional (commercial) implementations of MD simulations. In our approach, integration of the equations of motion is carried out in Cartesian coordinates, thus giving an exact definition of the kinetic energy and coupling. The classical equations of motion are formulated using our geometric statement function approach, which significantly reduces the number of mathematical operations required. Solution to these coupled differential equations is obtained numerically using

novel symplectic integrators developed in our laboratory which allow accurate integration for virtually any time scale [42].

We have developed an efficient MD-based method for simulating the condensation of polymer nano-particles with desired size [39–41]. The procedure starts by preparing a set of randomly coiled chains with a chosen chain length by propagating a classical trajectory to create a collision at the Cartesian origin. The collision creates a particle consisting of the six chains that are annealed to a desired temperature and rotated through a randomly chosen set of angles in three-dimensional space. Another set of six chains are propelled at the particle to create a particle with 600 more atoms. This process is continued until the desired size is reached. This method creates homogeneous particles that are in good agreement with 2-D diffraction observations on experimentally generated polymer particles. An example of a 20000 atom PE particle with chain lengths of 100 monomers is also shown in the Fig. 8.

4.1. Structural characteristics

Using the MD technique, various polymer particles with chain lengths of 1–200 monomers were generated with up to 300,000 atoms. To interpret the structural changes caused by the size-scale and shape of the particles, we first counted the surface atoms using a three-dimensional grid method in Cartesian coordinates. This allowed the ratio of the surface atoms to the total number of atoms to be obtained (the diameter is the average value of distance from a center of mass to the surface atoms). Since the smaller sized particles have more surface atoms than the larger ones (larger surface area to volume ratio), a decrease of the diameter increases the ratio as shown in Table 1. The large ratio of surface atoms to the total number of atoms leads to a reduction of the non-bonded interactions between the polymer chains on the surface layer, hence the cohesive energy is dramatically dependent on the size. In addition, the ratio of surface chain ends to total number of chain ends for the particles is much larger than that of the bulk system, leading to enrichment of chain ends at surface. This observation is consistent with analysis of thin films. With regard to an effect of the side chain atoms, the increase in these atoms corresponds to a decrease in the ratio of surface atoms and therefore represents an increase of cohesive energy of the system. The increase in cohesive energy is due to the increase in the number of atoms that are inside the spherical particle versus on the surface. This phenomenon is a result of the finite sized spherical confinement of the particle and is different than what is observed in the corresponding bulk systems (side chains tend to lower the cohesive energy).

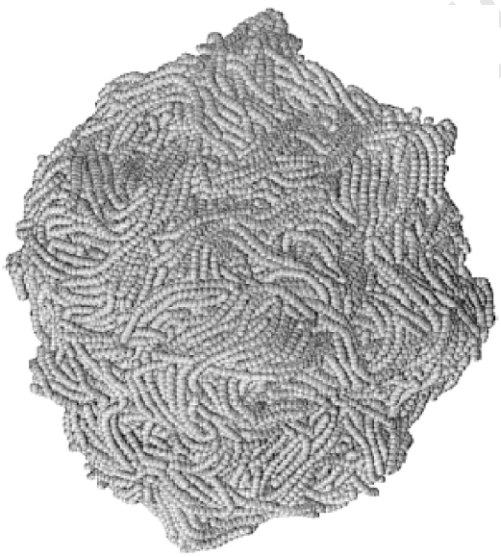

Fig. 8. Computed molecular structure of a 120,000 united atom polyethylene particle.

The surface area and volume were calculated using the contact-reentrant surface method (a spherical probe is used to trace molecular shape while in contact with the van der Waals surface) with a probe radii, $R_p = 1.4$ Å. The large proportional surface area defined by S_{ratio} = (surface area)/(volume) leads to large surface free energy, which is described by per unit of surface area (J/nm^2). The surface of the particles is also characterized by the fractal dimension that describes the degree of irregularity of the surface. The slope of the dependence of the surface area on the probe radius was calculated for probes in the range of 2.0 and 4.0 Å. The values of D are smaller for the particles than the value of the bulk ($D = 2.72$). This indicates that the surface is irregular and has many cavities that may introduce unique (catalytic or interpenetrating) properties of polymer particles. The free volume (cavities) and molecular packing can be important in a diffusion rate of a small molecule trapped in the particles. It also suggests that nano-scale polymer particles are loosely packed and can show dynamical flexibility (e.g. Compressive modulus of the particles is much smaller than that of the bulk system). The structural characteristics of the PE particles up to 120,000 atoms with a chain length of 100 united atoms are shown in Table 1.

Simulations were also performed on models for bulk polyethylene. The radial distribution function for the simulated bulk PE, which provides information on the intra and inter-molecular structure, was in very good agreement with experimental data. By comparing the bulk system with the nano-scale spherical particles, we can study the conformational changes of the particles due to the size reduction and the shape. Fig. 9 shows how the radial distribution function changes from the bulk simulation to that for particles of different sizes (a) and compositions (b) [43,44]. The most notable difference is in the amount of *gauche* conformations as signified by the magnitude of the peak at 3.2 Å. For the smaller particles this peak is almost entirely missing. The larger particles tend to have a somewhat higher concentration of *gauche* conformations but still significantly less than the bulk. This reduction in the

Table 1
Surface effects in polymeric particles

Polymer[a]	No. of backbone atoms	Diameter (nm)	Ratio of chain ends (%)	Surface area (nm^2)	Volume (nm^3)	S_{ratio} (nm^{-1})	Fractal dimension
PE	3,000	4.7	95	152	67	2.27	2.14
PE	6,000	5.6	87	257	138	1.86	2.15
PE	9,000	6.4	85	346	209	1.65	2.16
PE	12,000	7.0	83	443	279	1.55	2.16
PE	18,000	8.1	79	610	419	1.46	2.19
PE	24,000	9.0	76	814	564	1.44	2.21
PE	30,000	9.7	71	955	706	1.35	2.21
PE	60,000	12.4	69	1879	1424	1.32	2.26
PE	90,000	14.1	62	2765	2127	1.30	2.28
PE	120,000	16.1	60	4035	3128	1.29	2.28
PEP	3,000	4.9	85	190	86	2.22	2.19
PEP	6,000	6.1	81	327	175	1.87	2.21
PEP	9,000	7.0	81	478	264	1.81	2.22
PEP	12,000	7.7	74	568	354	1.60	2.25
aPP	3,000	5.3	77	235	105	2.24	2.21
aPP	6,000	6.8	75	416	214	1.94	2.21
aPP	9,000	7.3	74	604	322	1.88	2.24
aPP	12,000	7.9	70	780	431	1.81	2.28
PIB	3,000	6.3	75	332	131	2.53	2.25
PIB	6,000	7.2	72	683	262	2.60	2.28
PIB	9,000	8.2	71	948	399	2.38	2.32
PIB	12,000	9.1	68	1193	539	2.21	2.45

[a] PE = polyethylene, PEP = polyethylpropylene, aPP = atactic polypropylene, PIB = polyisobutylene1.

conformational disorder as the diameter of the particle decreases is a surface induced phenomenon. As the particle diameter decreases the surface area to volume ratio increases and the polymer chains are forced to lie mostly on the surface of the spherical particle. The surface tends to cause the polymer chains to form a pseudo crystalline layer, that is, the polymers fold in a nearly-all trans configuration.

Several simulations have been applied to study the morphology of single or multiple chains with different chain lengths and compositions [45], Since the surface chains of the PE nano-particles tend to straighten and align at temperatures below the melting point, the preferential morphology for the small PE particle with a long chain length is a rod-like shape. Liu and Muthukumar [46] also observed this mechanism in the simulations of polymer crystallization. This stretching of the chains leads to a reduction of the cohesive energy and an increase in volume. Studies on the effects of chain length show that the particles with the shortest chain length (see Fig. 10) have the most spherical shape.

4.2. Thermal and mechanical properties

Experimental measurements of a melting point (T_m) and glass transition temperature (T_g) are crucial properties that can be used to assess the physical state of a polymer. In our simulations, the melting point and the glass transition temperature can be obtained by calculating total energy and molecular volume of a system as a function of temperature. For a transition from the amorphous (solid) to the melt phase (liquid) and a glass–rubber transition, the volume increases owing to conformational disorder of the polymer particles. Energy, temperature, and volume are calculated while annealing the system gradually by scaling the momenta with a constant scaling factor. By computing the straight lines of molecular volume and total energy vs. temperature with a least squares fit, we can take the points where those extrapolated straight lines meet as the transition temperature T_m and T_g. We propagate the classical trajectories with the initial configurations of the steady state of the amorphous PE particle at a temperature of 450 K and schedule sampling until the temperature reaches 10 K.

Thermal analysis has provided a great deal of practical and important information about the molecular and material world relating to equations of state, critical points and the other thermodynamics quantities. Fig. 11(a) shows the dependence of the melting point and glass transition temperature on the diameter of the particle. The dramatic reduction of the melting point for the polymer particles is an important example of surface effects and shows the importance of size. Since the large ratio of surface atoms to the total number leads to a significant reduction of the non-bonded interactions (lower cohesive energy), the melting point decreases with decreasing size. Fig. 11(b)

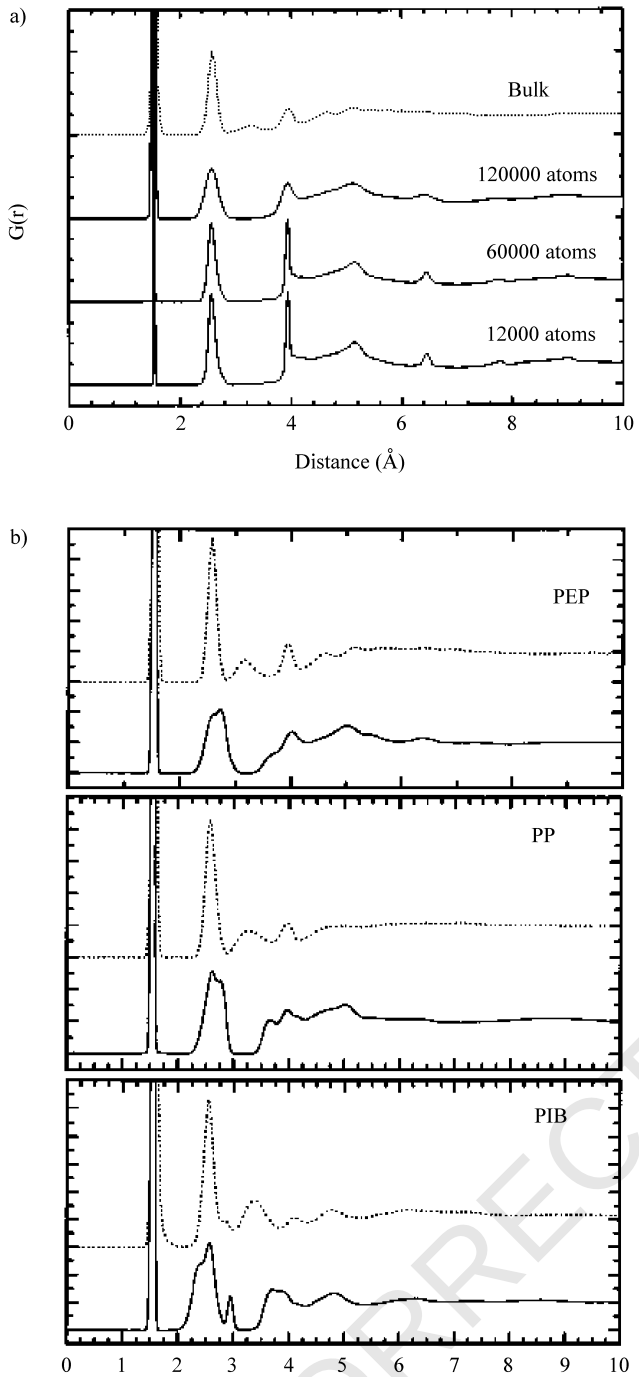

Fig. 9. (a) Radial distribution fuctions for bulk simulations of polyethylene compared to that of different sized particles. (b) Radial distribution functions for bulk (dashed) and polymer particles (solid) composed of different polymers.

shows the effect of chain length on these transition temperatures. A strong dependence of the melting point and the glass transition temperature on chain length is attributed to molecular weight and non-bonded energy of each chain. Some theoretical support for these observations comes from the Gibbs–Thompson equation which relates the difference in pressure at an interface to its surface

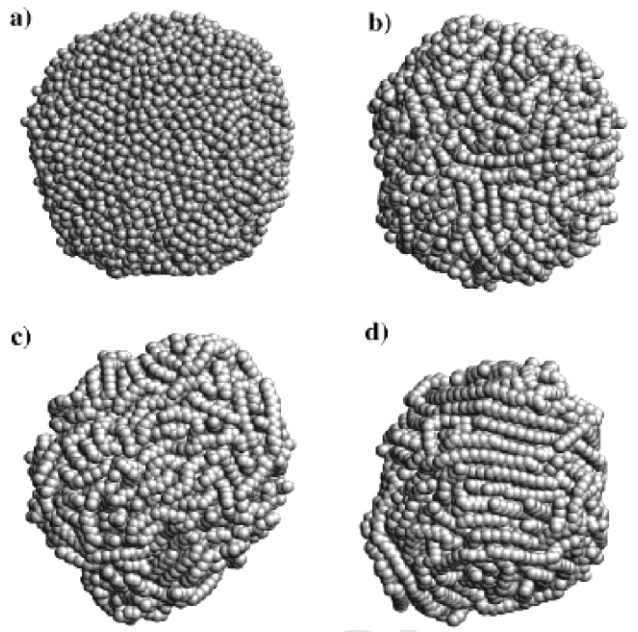

Fig. 10. Computed structures of polyethylene particles with different backbone chain lengths of (a) 1, (b) 10, (c) 50, (d) 100.

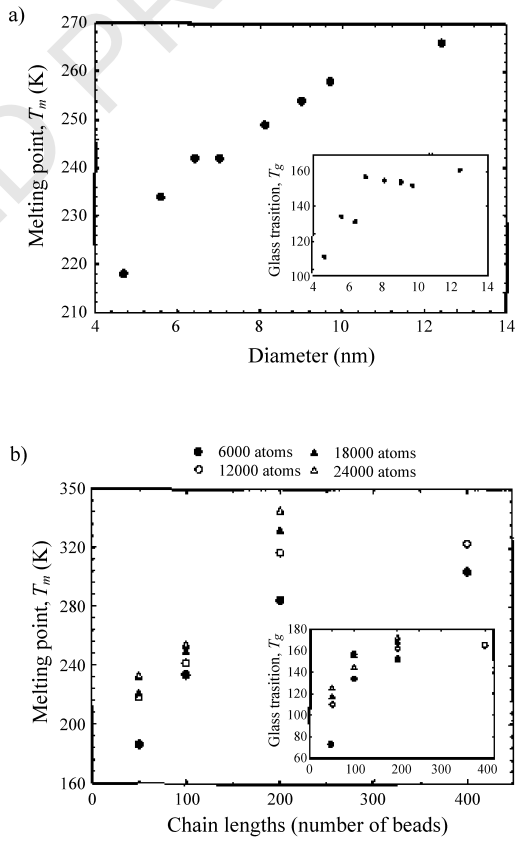

Fig. 11. (a) Melting point as a function of polymer particle diameter. The insert show results for the glass transition temperature. (b) Melting point as a function of the polymer backbone length. The Insert shows results for the glass transition temperature.

tension and curvature and can be used to predict a substantial reduction of the melting temperature for particles in the nano-size regime.

To investigate the atomistic mechanism of melting, the melting for the surface and inner chains of the particles were investigated as a function of size, chain length, and temperature by calculating molecular diffusion near the melting point for PE nano-particles. We selected the surface and inner chains for the PE particles, using a three-dimensional grid method in Cartesian coordinates to count surface atoms. Trajectories of center-of-mass for the surface and inner chains were calculated every picosecond to analyze the diffusion coefficient at a temperature. Diffusion coefficients for the surface and inner chains were computed from the mean-square displacements. The average mean-square displacement of center-of-mass for the chains can be determined and the diffusion constant (*D*rel) can be calculated from this curve using the Einstein relationship. The value of *D*rel for the surface chains is larger than one of the inner chains. For relatively low temperature (200 K), the diffusion of the particle with a chain length of 100 beads was not significantly changed. For temperatures above 200 K, however, the value for the surface chains rapidly increased. The higher diffusivity of the surface chains provides evidence that the melting starts from the surface of the PE particles, and the value of *D*rel increases as molecular weight decreases. From our thermodynamic analysis, the melting point of the particle (6000 atoms) with chain lengths of 50 and 100 beads was found to be 186 and 232 K, respectively. The melting point was higher than the temperature at which the surface chains experienced a significant change in mobility. A plot of *D*rel for the surface chains shows two steps during melting. The first step (mechanical melting) was at a temperature of 200 K and the second (thermodynamic melting) at 230 K. The first step is an early melting stage at which all chains in the particle start moving. The second step is the fusion stage of a solid. There is a plateau region between the first and second stages. The mobility of the chains in the outer layers increases rapidly after this region. In contrast, the chains in the core layer do not have the second step and mobility increase linearly. This observation provides evidence for a Lindermann1 [47] type mechanism of melting where surface melting of the nano-scale particle begins first. Other thermodynamic properties, such as entropy and Gibbs free energy for the polymer nano-particles have also been computed and are discussed in detail elsewhere [48].

The response of the polymeric particles to thermal stress demonstrates dramatic size dependence as discussed above. In a similar spirit, the response of these systems to applied mechanical stress was also investigated. In the past, numerous calculations have been performed for the mechanical property of bulk-like crystalline PE polymers using force field [49], semi-empirical [50], ab initio [51], and ab initio MD methods [52,53]. We have calculated the compressive (bulk) modulus for the amorphous polymer particles to get an idea of their stiffness and strength. The compressive modulus and yield point for the PE particles were investigated by applying an external force in MD simulations. It is known that values of the tensile modulus of bulk polyethylene are between 210 and 340 GPa [54] and the compressive modulus is generally higher than the tensile modulus [55]. In addition, the bulk and tensile strength or yield point are always much smaller than the modulus for a thermoplastic such as polyethylene. In the MD study of the polymer nano-particles, we observed a compressive modulus that is several orders of magnitudes smaller than the bulk values, and a yield point that was much larger than the modulus. The stress–strain curve actually looked more like that for an elastomer. However, the initial deformation caused by the compression (that which gives the modulus) is not reversible. What occurs during this phase is the deformation of a spherical particle to an oblate top. This structure is stable but it lies at a slightly higher energy than that for a spherical particle. Thus, the modulus for compression in this region is actually more a measure of the force required to deform the spherical polymer particle into an oblate top (pancake-like structure). Further deformation tends to be reversible up to the point of rupture. This deformation is actually more closely related to the bulk modulus since the stress is due to the cohesive energy and not a microstructure. This leads to a yield point that is significantly larger than the modulus.

4.3. Particle-surface interactions

In many of the submicron liquid droplet experiments, polymer particles were deposited on gold or glass microscope slides, and their morphology analyzed by scanning electron, optical, or phase contrast microscopy. For small sizes (1 μm), the particles formed a mixture of spheres and ‘pancake-like’ structures on a substrate. The droplet generator was normally mounted vertically and the polymer droplets ejected downward. The whole assembly and the particle free-falling region were shielded from room air current disturbance. We believe that a typical terminal velocity of a particle (due to the bouncy of air) is several meters per second (~1/100 Å/ps) in the droplet generator. Since a typical terminal velocity of a particle is several meters per second (~1/100 Å/ps) in the experiment, we believe the distortion of a particle (pancake) structure is mainly due to interactions between the particle and the substrate, and these interactions should be key to understanding polymer nucleation behavior on a substrate and wetting phenomenon for a liquid on surface. We used Nose–Hoover Chain (NHC) constant temperature MD to explore the behavior of a PE particle touching an Al substrate at a temperature of 200 K, which is below the melting point [39]. In the simulations, the surface was set at 5 Å from the closest atom in the particle Cartesian momenta were chosen with a random orientation in phase space and

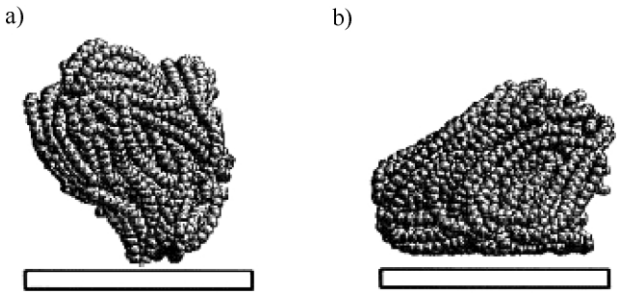

Fig. 12. The (a) initial and (b) final equilibrium structure of a polymer particle on a solid substrate.

magnitudes such that the total kinetic energy is the equipartition theorem expectation value. The area and asymmetry parameter of the PE particle of 3000 atoms with a chain length of 100 beads on a Al surface were compared to NHC MD without the surface interaction. It is clear that the particle is attracted to the surface and the shape is distorted. The asymmetry parameter indicates that the particle ends up with the shape of a prolate top (The surface chains of the particle of 3,000 atoms tend to straighten and align at temperatures below the melting point, hence the preferential shape is a prolate top (-0.6)). The initial and final structures are visualized in Fig. 12. The figure shows that the longest principle axis is parallel to the surface and the particle oriented in order to have the largest area in contact with the surface. Since the experimentally observed particles are much larger (1 m) than the simulated ones (4.7 nm), the surface tension is smaller and the distortion of the structure can be larger. From the particle collision studies [48], we found that the particles with the initial velocity less than 5 Å/ps self-organize into the spherical shape. In those collision simulations, the translational energy of the particles is much larger than the non-bonded interaction between the particle and the surface so that the particles can bounce back and subsequently reorganize their shape. Considering the morphology of the experimentally observed particles, we believe the main effect leading to the experimentally observed structure is the surface interaction between the polymer particles and the substrate.

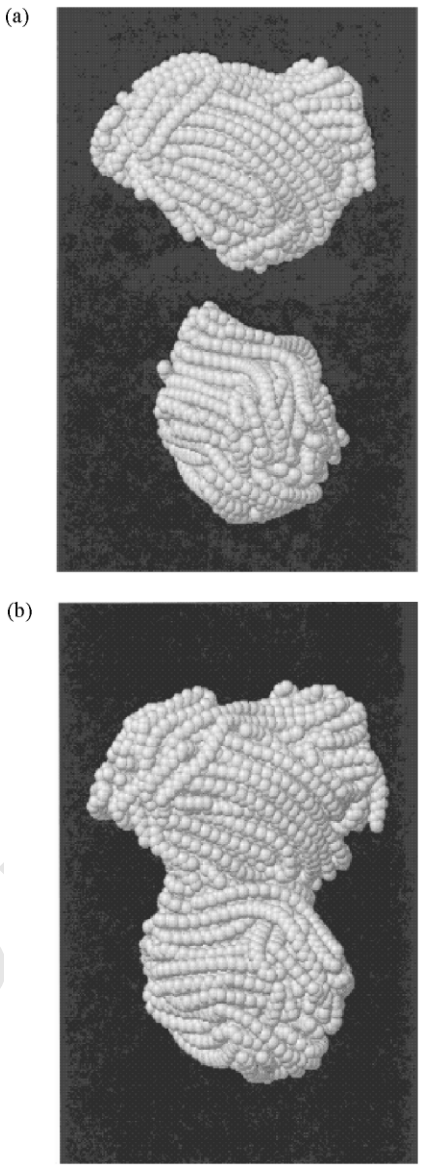

Fig. 13. The structure of two polymer particles (a) before collision and (b) following collision and equilibration.

4.4. Particle–particle interactions

As discussed in the previous sections of this paper, it has been observed that it is possible to construct well-defined and long-lived macrostructures composed of sequentially attached particles using a linear quadrapole as a particle positioning tool [30,34]. Physical measurements demonstrate that the polymer nano-particles retain much of their internal structure in the larger assembly. In essence, the larger superstructure is composed of a collection of polymer beads, each of which is itself a collection of smaller monomer units. However, the mechanism of attachment and binding is unclear. Phenomenological and atomistic studies of particle coalescence and annealing has shown that if collision times are shorter than the coalescence times, collisions of particles will result in the growth of single large particles, rather than a collection of smaller attached particles [56–58]. However, polymer chains of sufficient length may not migrate freely between the colliding particles, as do atoms in silica particles, inhibiting the reorganization of the collision cluster and leading to long coalescence times.

The microscopic details of polymer particle collision, merging, and chain transfer are quite interesting in their own right and have been explored recently by MD simulations. By simulating collisions of nanoscopic polymer particles (see Fig. 13), we found that the particles tend to agglomerate under a wide range of collision conditions. Only under very

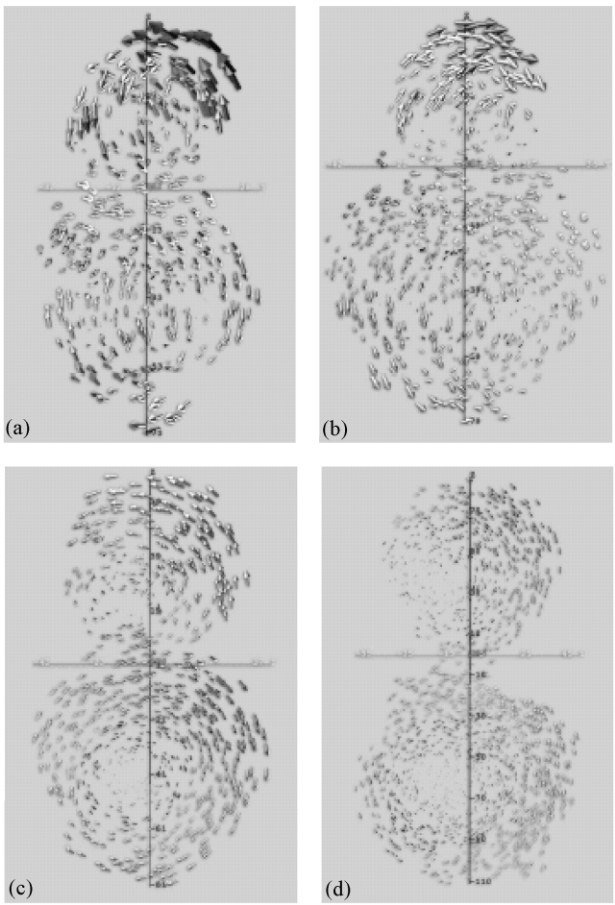

Fig. 14. Computed vibrational normal modes for various di-particle systems.

high energy collisions are the processes of particle fracture and chain exchange observed. Additional simulations have been carried out which have elucidated the nature of the vibrational normal modes of polymer particle structures [59,60]. The time averaged normal coordinate analysis method [61] was employed to find the vibrational frequencies and displacements of coupled polymer particle systems. A characteristic feature of the systems is the coupling of the rotational motions of individual particles to make low frequency gear-like modes (Fig. 14). While there is no true 'stretching' mode between polymer particles, due to extensive coupling to the internal elasticity of the particles, normal mode calculations indicate that vibrational frequencies of the quasi-stretching mode are related both to the mass of the particles and on the area of the interfacial region.

5. Conclusions and future

In this article, we have reviewed some of our recent progress and discussed new insights into generating, characterizing, and modeling of polymer micro and nano-particles. One of the main advantages of these materials is the observation that new dynamic behavior emerges when polymers are confined to small volumes of solution. Solvent evaporation in the droplet takes place on a time scale short enough to frustrate phase separation, producing polymer or polymer blend microparticles that are homogeneous within molecular dimensions. The structure and dynamics of the micro-confined polymer particles can be conveniently probed by conventional analytical techniques (such as Fraunhofer diffraction, fluorescence, and conventional phase-contrast microscopy). This capability allows production of useful polymer particles such as spherical polymer alloy microparticles with tunable properties, such as refractive index, simply by adjusting the relative weight fractions of the polymers in solution.

The combination of experimental evidence and computational modeling shows conclusively that stable, homogeneously blended (bulk-immiscible) mixed-polymer composites can be formed in a single microparticle of variable size. To our knowledge, this represents a new method for suppressing phase-separation in polymer blend systems without compatibilizers that allows formation of polymer composite micro- and nano-particles with tunable properties such as dielectric constant. In order to form homogeneous particles, conditions of rapid solvent evaporation (e.g. small [<10 μm] droplets or high vapor pressure solvents) and low polymer mobility must be satisfied. While this work obviously focused on polymeric systems, it should be pointed out that the technique is easily adaptable to making particles of small organic and inorganic (and hybrid composites) as well. A wide range of electronic, optical, physical and mechanical properties of single- and multi-component polymer nano-particles still remain to be explored.

To gain deeper insights into the structure, dynamics, and properties of polymeric micro- and nano-particles, we introduced an efficient method for atomistic modeling. Using MD, we have simulated nano-particles generated with up to 300,000 atoms with a variety of chain lengths and compositions. Our results show that the ratio of surface atoms to the total number of atoms for the polyethylene particles is very large, and the surface effects provide interesting properties that differ from the bulk systems. In particular, the melting point and glass transition temperature were found to be dramatically dependent on the size of the polymer particles. In addition, mechanical properties such as the compressive modulus of the PE particles appear to be significantly smaller than the value of the bulk, and the polymer particles appear to act more like an elastomer. It is well known that stress–strain properties are very sensitive to temperature, and an increase in temperature decreases the modulus. In the future study of mechanical properties of polymer nano- and micro-particles, we will analyze the dependence of the strength on size, temperature, chain length, and composition (multi-component blends). We are also extending this model to larger sized particles and

applying this method to model various polymers such as cyclic analogs and branched co-polymer systems.

Finally, polymer particle structures suggest the capability of manipulation of optical waves in a wide variety of 2- and 3-dimensional photonic wire structures that can be tailored to a particular application. We anticipate a number of interesting applications of these structures including 3-D conductive vertical wires/supports, and sensor technologies. By tuning the particle intersection (via adjustment of polymer blend composition), one can turn on (or off) coupling between orthogonal particle chain segments where the bend radius is close to the particle radius (e.g. 1–4 μm). Losses should be comparable to single- (linear) chain coupling which has already shown to be low. From a purely scientific point of view, photonic molecules represent a new field of study that incorporates a variety of disciplines including materials science, optics, and electronic structure. A number of challenges remain, however. Most polymeric materials are strongly absorbing at near infra-red (i.e. telecommunications) frequencies so it remains a non-trivial task to find polymer blend systems that are transmissive in this important frequency range but also retain the material properties similar to the PEG:PVA blend used in the studies summarized here. Further challenges include engineering an optical (or electronic) interface to the photonic molecule or polymer structure with specific frequency input-output requirements. This new class of structures may ultimately complement photonic bandgap crystal technology and add a new component in the toolbox for microphotonics.

Acknowledgements

This research was sponsored by the Division of Materials Sciences, Office of Basic Energy Sciences, US Department of Energy, under contract DE-AC05-00OR22725 with Oak Ridge National Laboratory, managed and operated by UT-Battelle, LLC. The authors would like to acknowledge collaborations with Drs R. Tuzun, K. Fukui, B. Mathorn, J. Ford, and C. Yang.

References

[1] Friend RH, Gymer RW, Homes AB, Burroughes JH, Marks RN, Taliani C, et al. Nature 1999;397:121–8.
[2] Hide F, Diazgarcia MA, Schwartz BJ, Heeger AJ. Acc Chem Res 1997;30:430–6.
[3] Srinivasarao M, Collings D, Philips A, Patel S. Science 2001;292:79.
[4] Gensler R, Groppel P, Muhrer V, Muller N. Particle Particle Syst Characterization 2002;19(5):293–9.
[5] Heeger AJ. J Phys Chem B 2001;105:8475.
[6] Feller JF, Linossier I, Grohens Y. Mater Lett 2002;57:64–71.
[7] Eisenberg P, Lucas JC, Williams RJJ. Macromol Symp 2002;189: 1–13.
[8] Pispisa B, Palleschi A. Macromolecules 1986;19:904–12.
[9] Liu TB, Burger C, Chu B. Prog Polym Sci 2003;28:5–26. and references cited therein.
[10] Jenekhe SA, Chen XL. Science 1998;279:1903–6.
[11] Jenekhe SA, Chen XL. Science 1999;283:372–5.
[12] Bates FS, Fredickson GH. Phys Today 1999;52:32–8.
[13] Thurn-Albrecht T, Schotter J, Kastle GA, Emley N, Shibauchi T, Krusin-Elbaum L, et al. Science 2000;290:2126–9.
[14] Kung C-Y, Barnes MD, Lermer N, Whitten WB, Ramsey JM. Appl Opt 1999;38:1481–7.
[15] Barnes MD, Ng KC, Fukui K, Sumpter BG, Noid DW. Macromolecules 1999;32:7183–9.
[16] Ng KC, Ford JV, Jacobson SC, Ramsey JM, Barnes MD. Rev Sci Instrum 2000;71(6):2497–9.
[17] Otaigbe JU, Barnes MD, Fukui K, Sumpter BG, Noid DW. Polym Phys Engng: Adv Polym Sci 2001;154:1–86.
[18] Ajito K, Torimitsu K. Trac-Trends Anal Chem 2001;20:255–62.
[19] Noid DW, Otaigbe JU, Barnes MD, Sumpter BG, Kung C.-Y. Apparatus for and method of producing monodisperse submicron polymer powders from solution, US Patent 6,461,546; Oct 8, 2002.
[20] Ford JV, Sumpter BG, Noid DW, Barnes MD, Hill SC, Hillis DB. J Phys Chem B 2000;104:495–502.
[21] Holler S, Surbek M, Chang RK, Pan YL. Opt Lett 1999;24:1185–7.
[22] Barnes MD, Lermer N, Whitten WB, Ramsey JM. Rev Sci Instrum 1997;2287-1.
[23] Koning C, van Duin M, Pagnoulle C, Jerome R. Prog Polym Sci 1998; 23:707–57.
[24] Yu JW, Douglas JF, Hobbie EK, Kim S, Han CC. Phys Rev Lett 1997; 78:2664–7.
[25] Marcus AH, Hussey DM, Diachun NA, Fayer MD. J Chem Phys 1996; 103:8189–200.
[26] Kung C-Y, Barnes MD, Lermer N, Whitten WB, Ramsey JM. App Opt 1999;38:1481–7.
[27] Barnes MD, Kung C-Y, Fukui K, Sumpter BG, Noid DW, Otaigbe JU. Opt Lett 1999;24:121–3.
[28] Fukui K, Sumpter BG, Barnes MD, Noid DW, Otaigbe JU. Macromol Theory Simul 1999;8:38–45.
[29] See for exampleMarshall L, Kra G. Opt Photon News 2002.
[30] Bayer M, Gutbrod T, Reithmayer JP, Forchel A, Reinecke TL, Knipp PA, Dremin AA, Kulakovskii VD. Phys Rev Lett 1998;81:2582.
[31] Barnes MD, Mahurin S, Mehta A, Sumpter BG, Noid DW. Phys Rev Lett 2002;88:015508.
[32] Ng KC, Ford JV, Jacobson SC, Ramsey JM, Barnes MD. Rev Sci Instrum 2000;71:2497.
[33] Videen G, Ngo D, Hart MB. Opt Commun 1996;125:275.
[34] Moon H-J, Kim G-H, Lim Y-S, Go C-S, Lee J-H, Chang J-S. Opt Lett 1996;21:913.
[35] Mahurin S, Mehta A, Sumpter BG, Noid DW, Runge K, Barnes MD. Opt Lett 2002;27:610.
[36] Chang S, Chang RK, Stone AD, Nockel JU. J Opt Soc Am B 2000;17: 1828.
[37] Hayashi C, Uyeda R, Tasaki A. Ultra fine particles technology. New Jersey: Noyes; 1997.
[38] Ichinose N, Ozaki Y, Kashu S. Superfine particle technology. London: Springer-Verlag; 1992.
[39] Fukui K, Sumpter BG, Barnes MD, Noid DW, Otaigbe JU. Macromol Theory Simul 1999;8:38–45.
[40] Fukui K, Sumpter BG, Runge K, Kung CY, Barnes MD, Noid DW. Chem Phys 1999;244:339–49.
[41] Fukui K, Sumpter BG, Barnes MD, Noid DW. Comput Theor Polym Sci 1999;9:245–54.
[42] Gray SK, Noid DW, Sumpter BG. J Chem Phys 1994;101:4062–72.
[43] Fukui H, Sumpter BG, Barnes MD, Noid DW. Macromolecules 2000; 33:5982.
[44] Fukui K, Sumpter BG, Barnes MD, Noid DW. Polymer J 1999;31: 664.
[45] Tanaka G, Mattice WL. Macromolecules 1995;28:1049.
[46] Liu C, Muthukumar M. J Chem Phys 1995;103:9053.
[47] Lindemann FA. Z Phys 1910;14:609.

[48] Fukui K, Sumpter BG, Noid DW, Yang C, Tuzun RE. J Polym Sci B Polym Phys 2000;38:1812.
[49] Brown D, Clarke JHR. Macromolecules 1991;24:2075.
[50] Hor T, Adams W, Pachter R, Haaland P. Polymer 1993;34:2481.
[51] Crist B, Herena PG. J Polym Sci B Polym Phys 1996;34:449.
[52] Meier RJ. Macromolecules 1993;26:4376.
[53] Hageman JCL, Meier RJ, Heinemann M, de Groot RA. Macromolecules 1997;30:5953.
[54] Shoemaker J, Horn T, Haaland P, Pachter R, Adams WW. Polymer 1992;33:33351.
[55] Nielen LE. Mechanical properties of polymers and composites. New York: Marcel Dekker; 1974.
[56] Hathorn BC, Sumpter BG, Barnes MD, Noid DW. J Phys Chem B 2001;105:11468.
[57] Hathorn BC, Sumpter BG, Barnes MD, Noid DW. Polymer 2002;43:3115.
[58] Hathorn BC, Sumpter BG, Noid DW, Barnes MD. Macromolecules 2002;35:1102.
[59] Hathorn BC, Sumpter BG, Noid DW, Yang C, Tuzun RE. J Phys Chem B 2002;106:9174.
[60] Hathorn BC, Sumpter BG, Noid DW, Yang C, Tuzun RE. Polymer 2003;44:3761.
[61] Noid DW, Fukui K, Sumpter BG, Yang C, Tuzun RE. Chem Phys Lett 2000;316:285.

Dr. Bobby Sumpter received his Bachelor of Science in Chemistry from Southwestern Oklahoma State University (1983) with minors in Mathematics, Physics, Computer Science, and Geology. He received a Ph.D. in Physical Chemistry from Oklahoma State University in 1986. Following postdoctral studies in Chemical Physics at Cornell University 1987-1988 and in polymer chemistry at the University of Tennessee, Bobby joined the Chemistry Division at Oak Ridge National Laboratory in the Polymer Science group. He serves as an Advisory Committee Member on the *International Journal of Smart Engineering System Design*, is a continuing Co-organizer (organization committee) of the annual international meeting, *Artificial Neural Networks in Engineering*, and Co-organized and Chaired the *1st DOE Workshop on Applications of Neural Networks in Materials Science* (Feb 28–March 2, 1994).

Dr. Donald W. Noid received his Ph.D. in theoretical chemistry in 1976 from the University of Illinois under the guidance of Professor R. A. Marcus, Nobel Laureate. After a year as an NSF energy-related Postdoctoral Fellow working on picosecond laser experiments at the University of Illinois, he accepted a Eugene Wigner Fellowship and staff position at Oak Ridge National Laboratory. In 1981 he became an adjunct Professor in the Chemistry Department at The University of Tennessee - Knoxville. In 1983 he was on sabbatical in the Theoretical Chemistry Institute at the University of Wisconsin as the Theoretical Institute Fellow and Visiting Associate Professor. Dr. Noid was a visiting senior scientist at the Institute of Defense Analysis for a one-year period in 1985-1986. He has also served as a consultant to various organizations, including the Advanced Isotope Separation Group at K-25, Physical Sciences Inc., ALZA Corporation and YAHSGS.

Dr. Mike Barnes received the B.S. degree in Chemistry from California State University, Sonoma in 1985 and the Ph.D. in Chemistry from Rice University in 1991 under the supervision of Philip R. Brooks and Robert F. Curl. He was a postdoctoral associate at Oak Ridge National Laboratory with J. Michael Ramsey in the Chemical Sciences Division from 1991 to 1994, where he developed techniques for probing single fluorescent molecules and novel optical physics in isolated microdroplets of solution. In collaboration with Bobby Sumpter and Don Noid, currently in the Computer Sciences and Mathematics Division at ORNL, the research focus is using ink-jet printing techniques to prepare micron- and nanoscale polymeric species with novel optical and material properties.